4 Theoretical Cardiac Electrophysiology

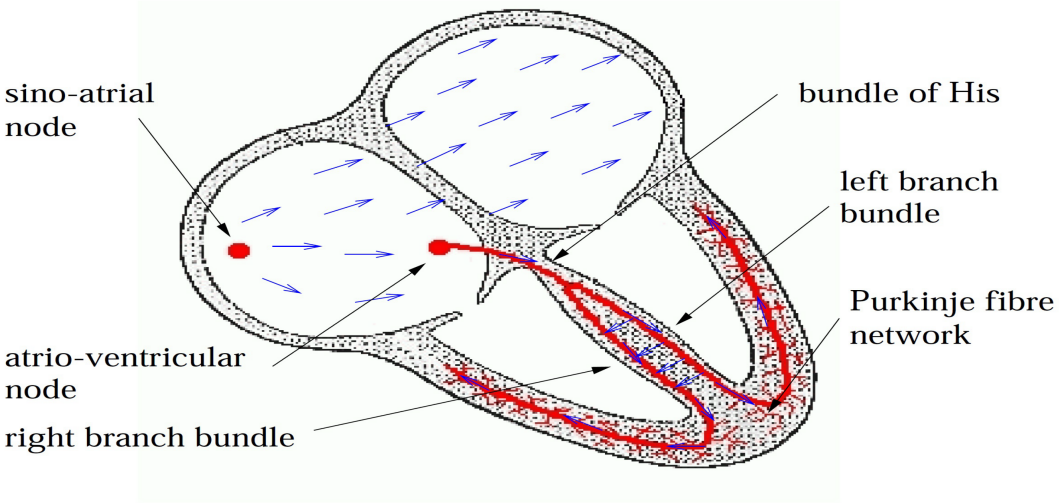

Figure 1: A schematic of the electrophysiological wave propagation in the heart. The blue arrows show the direction of the electric signal and the red curves are the Purkinje fibre network, a major conduit of the electrophysiological pulse (adapted from Houghton & Gray 1997). The ventricles are the lower chambers in the schematic: the blood that accumulates in the left ventricle in each heart beat is oxygenated and pumped around the body, the blood that accumulates in the right ventricle is pumped through the lungs for oxygenation.

An electrophysiological cell membrane potential oscillation in *pacemaker* cells, analogous to that seen in the Fitzhugh-Nagumo equations, initiates a cell membrane action potential in the cells of the heart sino-atrial node. This in turn initiates a propagating pulse of membrane potential through cardiac muscle fibres, which drives a muscular contraction, ultimately pumping blood. The electrophysiological details are broadly the same as nerve cells, though additional ions such as calcium are involved, and the waves occur in higher spatial dimensions.

These electrophysical waves can be modelled at numerous levels of detail. A common simple model is to represent the cardiac muscle fibre membrane potential via a Fitzhugh-Nagumo approximation. With the intracellular and extracellular resistances taken to be constant, as with r_i and r_e in the one dimensional derivation summarised in §2.1, the non-dimensional Fitzhugh-Nagumo equations take the form

$$\begin{aligned} \varepsilon\frac{\partial v}{\partial \tau} &= \varepsilon^2\nabla^2 v + Av(v-a)(1-v) - w + I^*, \\ \frac{\partial w}{\partial \tau} &= -w + bv, \end{aligned} \tag{1}$$

where $\varepsilon \ll 1,\ A \sim O(10),\ 0 < a < 1$ and $b \sim O(1)$ is sufficiently large to ensure there is only one homogeneous steady state.

Such models qualitatively give broadly the correct behaviour for understanding many biophysical principles. However, the fine electrophysiological details are neglected as is the fact the cardiac cell membrane potential propagates more readily along cardiac muscle fibres rather than perpendicular to them.

A blockage in the electrophysiological conduction of the cell membrane potential wave leads to aberrant behaviour such as spiral waves, which manifest clinically as ventricular tachycardia, and can readily breakdown with chaotic behaviour, or ventricular fibrillation, which is rapidly fatal. Similarly anomalous pacemaking behaviour can occur in regions, known as ectopic foci, which are away from the sino-atrial node: this is potentially dangerous in that a propagating pulse of membrane potential can be initiated, which interferes with normal cardiac function. Below we explore pacemakers, an ectopic focus and spiral waves in more detail.

4.1 Pacemakers - *Optional*

The pacemaker cells in the heart sino-atrial node undergo cell membrane potential oscillations. In a non-dimensional spatially homogeneous Fitzhugh Nagumo representation

$$\varepsilon \frac{dv}{d\tau} = Av(v-a)(1-v) - w + I^*, \quad \frac{dw}{d\tau} = -w + \frac{b}{\varepsilon}v,$$

we have the equilibrium point occurs on the second branch of the cubic nullcline for oscillatory behaviour:

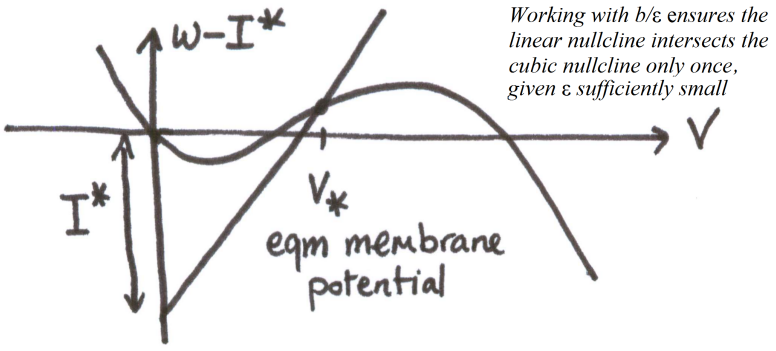

In particular, with $f(v) = Av(a-v)(1-v)$ and v_* the equilibrium potential, we have $f'(v_*) > 0$; from the exercise sheet 1, problem 3, one requires $f'(v_*) > \varepsilon$.

Suppose we have a heterogeneous tissue, with a cluster of pacemaker cells in region Ω_1 and excitable cells in the rest of the region, which we take to be the surface of a sphere for simplicity. We model this by first considering the spatially varying Fitzhugh Nagumo equations where

$$\varepsilon\frac{dv}{d\tau} = \varepsilon^2\nabla^2 v + Av(v-a)(1-v) - w + I^*(\mathbf{x}), \quad \frac{dw}{d\tau} = -w + \frac{b}{\varepsilon}v,$$

with

$$I^*(\mathbf{x}) = \begin{cases} I_0^* & \mathbf{x} \in \Omega_1 \\ 0 & \text{otherwise} \end{cases}$$

We ask whether the pacemaking cells can initiate an electrophysiological disturbance in the surrounding excitable tissue; for instance whether a small ectopic focus can invoke an aberrant electrophysiological wave.

Let $v_0(\mathbf{x}), w_0(\mathbf{x})$ denote the solutions of the steady state problem:

$$0 = \varepsilon^2\nabla^2 v_0 + Av_0(v_0-a)(1-v_0) - w_0 + I^*(\mathbf{x}), \quad 0 = -w_0 + \frac{b}{\varepsilon}v_0.$$

We consider linear stability, writing

$$v(\mathbf{x}) = v_0(\mathbf{x}) + V(\mathbf{x})e^{\lambda\tau/\varepsilon}, \quad w(\mathbf{x}) = w_0(\mathbf{x}) + W(\mathbf{x})e^{\lambda\tau/\varepsilon}.$$

Substituting this into the original equations and linearising gives:

$$\lambda V = \varepsilon^2\nabla^2 V + f'(v_0(\mathbf{x}))V - W, \quad \lambda W = \varepsilon\left(\frac{b}{\varepsilon}V - W\right).$$

Eliminating W gives

$$\varepsilon^2\nabla^2 V + f'(v_0(\mathbf{x}))V = EV, \quad E = \lambda + \frac{b}{\lambda+\varepsilon},$$

and an eigenvalue problem, which determines E.

We immediately have that E is real, as ∇^2 is self-adjoint. Further,

$$\lambda^2 - (E-\varepsilon)\lambda + (b - \varepsilon E) = 0$$

and hence (given $\varepsilon \ll b$) we have $E < \varepsilon$ is sufficient to have $\mathrm{Re}\lambda < 0$ and thus linear stability.

Except for a diffusive boundary layer at the edge of Ω_1, of width $\sqrt{\varepsilon}$, we have the steady solutions $v_0,\ w_0$ will be essentially constant, taking values associated with a pacemaker in the interior of Ω_1 and excitable cells elsewhere. Hence, apart from within the thin boundary layer, we have

$$f'(v_0(\mathbf{x}))$$

is given by the analogous value from the homogeneous problem for the pacemaker cells in region Ω_1 and similarly for the excitable cells outside Ω_1. The former is positive, the latter negative.

In the following problem, we explore this model further to demonstrate that it predicts a critical mass of oscillatory cells is required to drive the medium away from its homogeneous steady state.

1. Suppose we have a heterogeneous tissue, with a cluster of pacemaker cells in region Ω_1 and excitable cells in the rest of the region, which we take to be the surface of a sphere for simplicity. We model this by first considering the non-dimensional spatially varying Fitzhugh Nagumo equations where

$$\varepsilon\frac{dv}{d\tau} = \varepsilon^2\nabla^2 v + f(v) - w + I^*(\mathbf{x}), \quad \frac{dw}{d\tau} = -w + \frac{b}{\varepsilon}v,$$

with

$$f(v) = Av(v-a)(1-v), \qquad I^*(\mathbf{x}) = \begin{cases} I_0^* & \mathbf{x} \in \Omega_1 \\ 0 & \text{otherwise} \end{cases},$$

with $0 < \varepsilon \ll a \ll 1$, $b \sim \mathrm{O}(1)$, $A \sim \mathrm{O}(1)$.

Conducting a linear stability analysis reveals that the steady state of the above problem, $v_0(\mathbf{x})$, $w_0(\mathbf{x})$, is linearly stable when $\mathrm{Re}\lambda < 0$ for all non-trivial solutions of the following eigenvalue problem for E:

$$\varepsilon^2\nabla^2 V + f'(v_0(\mathbf{x}))V = EV, \quad E = \lambda + \frac{b}{\lambda+\varepsilon}.$$

Show that E is real, and hence that $E < \varepsilon$ is sufficient for linear stability. Further show that there is a Hopf bifurcation as E increases through ε.

By considering a spherical harmonic expansion of V in the two cases where (i) all cells are excitable and (ii) all cells are oscillatory, explain why a critical mass of oscillatory cells is required to drive the medium away from its homogeneous steady state. [*Assume that the spherical harmonics are complete and that V is sufficiently smooth to be represented by a spherical harmonic expansion*].

4.2 Cardiac Waves and The Geometric Theory of Wave propagation

Below we explore Fitzhugh-Nagumo waves in more than one spatial dimension, taking advantage of the fact the spatial scales normal to the wavefront are much less than that of the domain or the extent of the wave tangential to the front (see figure 2). We will derive the *eikonal* equation, linking curvature and normal velocity of the excitation front.

We will find that the curvature of the transition region is crucial in our studies below, and hence we start by investigating the notion of curvature. Following this we will investigate how to extract equations for the propagation of transition regions from the partial differential equation in question.

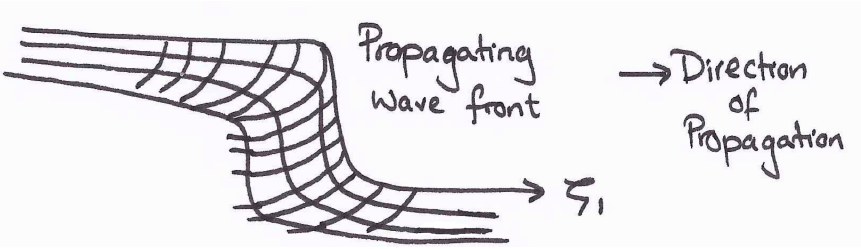

Figure 2: Propagating wavefront. The spatial scales normal to the wavefront are much less than that of the domain or the extent of the wave tangential to the front.

4.2.1 Curvature

The magnitude of the curvature of a *two-dimensional* surface at a point P is the reciprocal of the radius of the best fit circle to the surface at P (see figure 3). We seek an expression for the curvature in terms of the unit normal at P.

Defining the 2D surface by $z = h(x)$, we first find the unit normal and unit tangent vectors:

$$\mathbf{n} = \frac{(-h', 1)}{(1 + h'^2)^{1/2}}, \qquad \mathbf{t} = \frac{(1, h')}{(1 + h'^2)^{1/2}},$$

where here primes denote differentiation with respect to x.
Important The normal, $\mathbf{n}$, is defined off surface by enforcing that it is independent of the direction perpendicular to the surface. We then define the curvature to be

$$\kappa = \nabla \cdot \mathbf{n} = \frac{d}{dx}\left(\frac{-h'}{(1 + h'^2)^{1/2}}\right) = -\frac{h''}{(1 + h'^2)^{3/2}}.$$

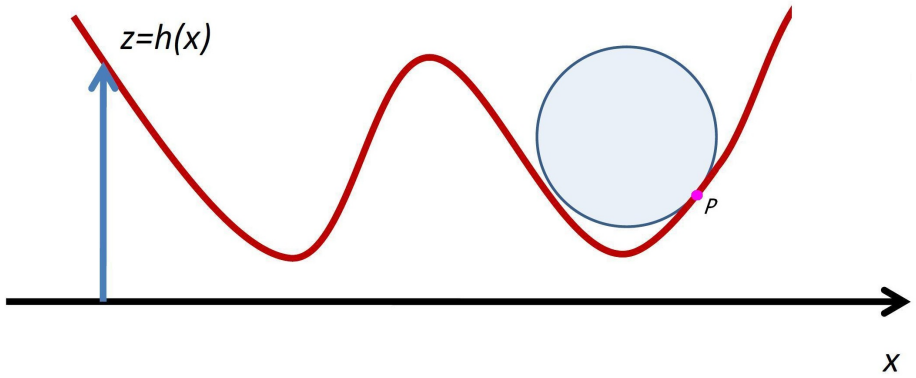

Figure 3: Curvature.

An alternate expression for the curvature in 2D is as follows. Consider a line given by $(x, y) = (X(s), Y(s)),\ s \in [0, \infty)$; *i.e.* it is parameterised by s. If we express the line in the form $y = h(x)$,

then $h' = Y'(s)/X'(s)$ and hence we have

$$\kappa = -\frac{h''}{(1+h'^2)^{3/2}} = \frac{-Y'(s)X''(s) + X'(s)Y''(s)}{(X'^2(s) + Y'^2(s))^{3/2}}.$$

In *three* dimensions we define the curvature to be

$$\kappa = \nabla \cdot \mathbf{n} = -\frac{h_{xx} + h_{yy}}{(1 + h_x^2 + h_y^2)^{3/2}},$$

with an intuitive justification analogous to the above.

4.2.2 Geometric Theory of Wave propagation: The Eikonal Equation

In this section a geometrical theory of wave propagation is introduced which allows the study of wave propagation in more than one dimension. The theory is based on the assumption that the width of the wavefront is small compared with the radius of curvature of the wavefront. The ionic currents are modelled using the FitzHugh-Nagumo equations, and we again consider the limit $\varepsilon \to 0$.
The Fitzhugh-Nagumo equations (1) in more than spatial dimension are (where here we set $I^* = 0$)

$$\begin{aligned} \varepsilon \frac{\partial v}{\partial t} &= \varepsilon^2 \frac{\partial^2 v}{\partial x_i \partial x_i} + Av(v-a)(1-v) - w \\ \frac{\partial w}{\partial t} &= -w + bv. \end{aligned} \tag{2}$$

Planar wavefront

We define the wavefront to be the region where the membrane potential v changes rapidly, and is of $O(\varepsilon)$ in the space variable. We define the unit normal to the wavefront as $\mathbf{n}$, and consider first the case where $\mathbf{n}$ is a constant vector.

We introduce the travelling wave co-ordinate $\xi = (\mathbf{x}.\mathbf{n} - ct)/\varepsilon$, and look for solutions of (2) of the form $v = V(\xi)$, $w = W(\xi)$. Then

$$V'' + cV' + f(V) - W = 0, \quad W' = 0, \tag{3}$$

where now primes denote differentiation with respect to ξ, $f(V) = AV(V-a)(1-V)$ and

$$V(\xi) \to 1 \qquad \text{as} \qquad \xi \to -\infty, \tag{4}$$

$$V(\xi) \to 0, W(\xi) \to 0 \qquad \text{as} \qquad \xi \to \infty, \tag{5}$$

where the latter condition on W arises since the recovery variable w is zero ahead of the wave. Hence, $W \equiv 0$, and the governing equation for V is simply

$$V'' + cV' + f(V) = 0. \tag{6}$$

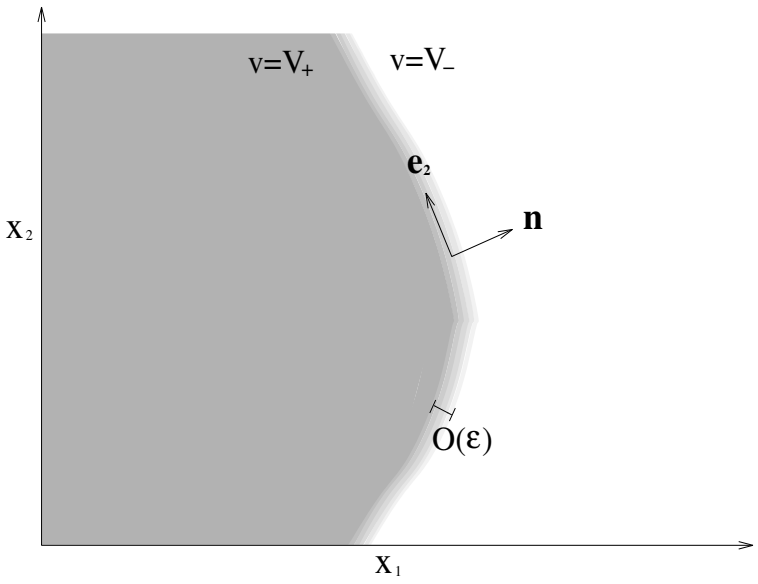

Figure 4: A schematic diagram of the membrane potential in a 2-dimensional wavefront. The potential is represented by the shade (dark=high potential; light=low potential). The wavefront has $O(1)$ curvature and is of width $O(\varepsilon)$. Note that for $f(v) = Av(v-1)(1-v)$ we have $V^+ = 1$ and $V^- = 0$.

Note that the form of f is such that a travelling wave solution exists with $c > 0$ (see §2.1.1). These solutions correspond to *planar* wavefronts propagating in the direction $\mathbf{n}$. Note that in the region of the wavefront $\mathbf{n}.\nabla v = O(\varepsilon^{-1})$.

Nonplanar wavefronts

We now consider curved wavefronts in three dimensions where the radius of curvature is $O(1)$ and the width of the wavefront is $O(\varepsilon)$. A useful picture of this approximation is to consider the wavefront as the skin of an inflated balloon which is thin compared with the radius of the balloon. A surface may be considered by introducing a generalised co-ordinate transformation

$$\mathbf{x} = \mathbf{x}(\bar{\mathbf{x}}, \bar{t}) \qquad \text{and} \qquad t = \bar{t}, \tag{7}$$

such that the wavefront is the surface $\bar{x}_1 = 0$, and $\bar{x}_2$ and $\bar{x}_3$ are coordinates that parameterise the surface. We now define tangent vectors $\mathbf{e}_i$

$$\mathbf{e}_i = \frac{\partial \mathbf{x}}{\partial \bar{x}_i}. \tag{8}$$

The tangent vectors are orthogonal, so we can write $\mathbf{e}_1 = \mathbf{e}_2 \times \mathbf{e}_3$ etc. Additionally, $\mathbf{e}_1$ is normal

to the surface, and vectors $\mathbf{e}_2$ and $\mathbf{e}_3$ lie tangent to the surface. We let $\mathbf{n} = a\mathbf{e}_1$ were a is a normalisation factor, and demand that $|\mathbf{n}| = 1$, which gives $a = \mathbf{e}_1.(\mathbf{e}_2 \times \mathbf{e}_3)$ (see figure 4).
We now consider how the derivatives transform

$$\frac{\partial}{\partial \bar{x}_i} = J_{ij}\frac{\partial}{\partial x_j} \qquad \text{and} \qquad \frac{\partial}{\partial \bar{t}} = \frac{\partial}{\partial t} + \frac{\partial x_j}{\partial \bar{t}}\frac{\partial}{\partial x_j}, \tag{9}$$

where J is the Jacobian matrix

$$J_{ij} = \frac{\partial x_j}{\partial \bar{x}_i} \qquad \Rightarrow \qquad \mathbf{J} = \left(\begin{array}{c} \mathbf{e}_1^{\mathrm{T}} \\ \hline \mathbf{e}_2^{\mathrm{T}} \\ \hline \mathbf{e}_3^{\mathrm{T}} \end{array}\right). \tag{10}$$

The inverse transforms are then given by

$$\frac{\partial}{\partial x_i} = J^{-1}_{ij}\frac{\partial}{\partial \bar{x}_j} \qquad \text{and} \qquad \frac{\partial}{\partial t} = \frac{\partial}{\partial \bar{t}} - \frac{\partial x_i}{\partial \bar{t}}J^{-1}_{ij}\frac{\partial}{\partial \bar{x}_j}, \tag{11}$$

where J^{-1}_{ij} is the inverse of J and is given by

$$\begin{aligned} \mathbf{J^{-1}} &= \left(\frac{\mathbf{e}_2 \times \mathbf{e}_3}{\mathbf{e}_1.(\mathbf{e}_2 \times \mathbf{e}_3)}\middle|\, \frac{\mathbf{e}_3 \times \mathbf{e}_1}{\mathbf{e}_1.(\mathbf{e}_2 \times \mathbf{e}_3)}\middle|\, \frac{\mathbf{e}_1 \times \mathbf{e}_2}{\mathbf{e}_1.(\mathbf{e}_2 \times \mathbf{e}_3)}\right), & (12)\\ &= (\mathbf{n}|\ \mathbf{e}_3 \times \mathbf{n}|\ \mathbf{n} \times \mathbf{e}_2), & (13)\end{aligned}$$

where we have used the properties of $\mathbf{e}_1$. The transform of the Laplacian is

$$\nabla^2 v = J^{-1}_{ij}J^{-1}_{ik}\frac{\partial^2 v}{\partial \bar{x}_j \partial \bar{x}_k} + \left(\frac{\partial}{\partial x_i}J^{-1}_{ik}\right)\frac{\partial v}{\partial \bar{x}_k}, \tag{14}$$

where the matrix product $J^{-1}_{ij}J^{-1}_{ik}$ is

$$J^{-1}_{ij}J^{-1}_{ik} = \left((\mathbf{J^{-1}})^T\mathbf{J^{-1}}\right)_{jk} = \begin{pmatrix} 1 & 0 & 0 \\ 0 & b_{22} & b_{23} \\ 0 & b_{32} & b_{33} \end{pmatrix}, \tag{15}$$

where b_{ij} depend upon the details of the transformation, however are not required in our calculation. Next we define the stretched variable $\xi = \bar{x}_1/\varepsilon$ and seek a solution the form $v(\xi, \bar{x}_2, \bar{x}_3, \bar{t}) = V(\xi)$ (with a similar form for w), so (14) becomes

$$\begin{aligned} \nabla^2 v &= \frac{1}{\varepsilon^2}J^{-1}_{i1}J^{-1}_{i1}\frac{d^2V}{d\xi^2} + \frac{1}{\varepsilon}\left(\frac{\partial}{\partial x_i}J^{-1}_{i1}\right)\frac{dV}{d\xi}, & (16)\\ &= \frac{1}{\varepsilon^2}\frac{d^2V}{d\xi^2} + \frac{1}{\varepsilon}\nabla.\mathbf{n}\frac{dV}{d\xi}, & (17)\end{aligned}$$

and (11) becomes

$$\frac{\partial v}{\partial t} = -\frac{1}{\varepsilon}\frac{\partial x_i}{\partial \bar{t}} J^{-1}_{i1} \frac{dV}{d\xi}, \tag{18}$$

$$= -\frac{1}{\varepsilon}\frac{\partial \mathbf{x}}{\partial \bar{t}}.\mathbf{n}\frac{dV}{d\xi}. \tag{19}$$

Inserting (17) and (19) into (2) yields

$$\frac{d^2V}{d\xi^2} + \left(\frac{\partial \mathbf{x}}{\partial \bar{t}}.\mathbf{n} + \varepsilon \nabla.\mathbf{n}\right)\frac{dV}{d\xi} + f(V) - W = 0, \ \frac{dW}{d\xi} = 0. \tag{20}$$

As before, matching to the form of w ahead of the wave we see $W \equiv 0$. Then equation (20)a is the same form as the travelling wave equation (3) if

$$c = \frac{\partial \mathbf{x}}{\partial \bar{t}}.\mathbf{n} + \varepsilon \nabla.\mathbf{n}. \tag{21}$$

The travelling wave equation (3) (with $W = 0$) had a solution $V(\xi; c)$ on the interval $(-\infty, \infty)$ corresponding to wavefronts travelling with velocity c: this is the speed of the *planar* (one-dimensional) travelling wave solutions, and from §2.1.1, we have that

$$c = \sqrt{\frac{A}{2}}(1 - 2a). \tag{22}$$

Equation (21) is called the eikonal-curvature equation: the first term on the r. h. s. is the localised speed of the wavefront and the second term is proportional to the curvature of the wavefront. The second term describes how the wave speed is reduced by curvature.

Consider wave propagation in two-dimensions so that the wavefront is a line which evolves with time. In general the position of the wavefront can be written in the form

$$\mathbf{x}(s;t) = \begin{pmatrix} X(s;t) \\ Y(s;t). \end{pmatrix} \tag{23}$$

Inserting (23) into (21) and carrying out a change of variables (Example sheet 4, question 2) yields the eikonal-curvature equation for evolution of a generalised wavefront in two-dimensions:

$$c = \frac{X_t Y_s - Y_t X_s}{(X_s^2 + Y_s^2)^{1/2}} + \varepsilon \frac{Y_{ss} X_s - X_{ss} Y_s}{(X_s^2 + Y_s^2)^{3/2}}. \tag{24}$$

In the following sections we will look at solutions of this equation which gives rise to wavefronts with different geometries.
NB. We must not drop the $\varepsilon \nabla \cdot \mathbf{n}$ term at leading order for non-planar dynamics; non-trivial solutions do occur when $\nabla \cdot \mathbf{n} \sim O(1/\varepsilon)$.
We can use the eikonal equation to show that a front of a plane wave solution of equation (20) is stable with respect to small perturbations that distort the front, as follows.

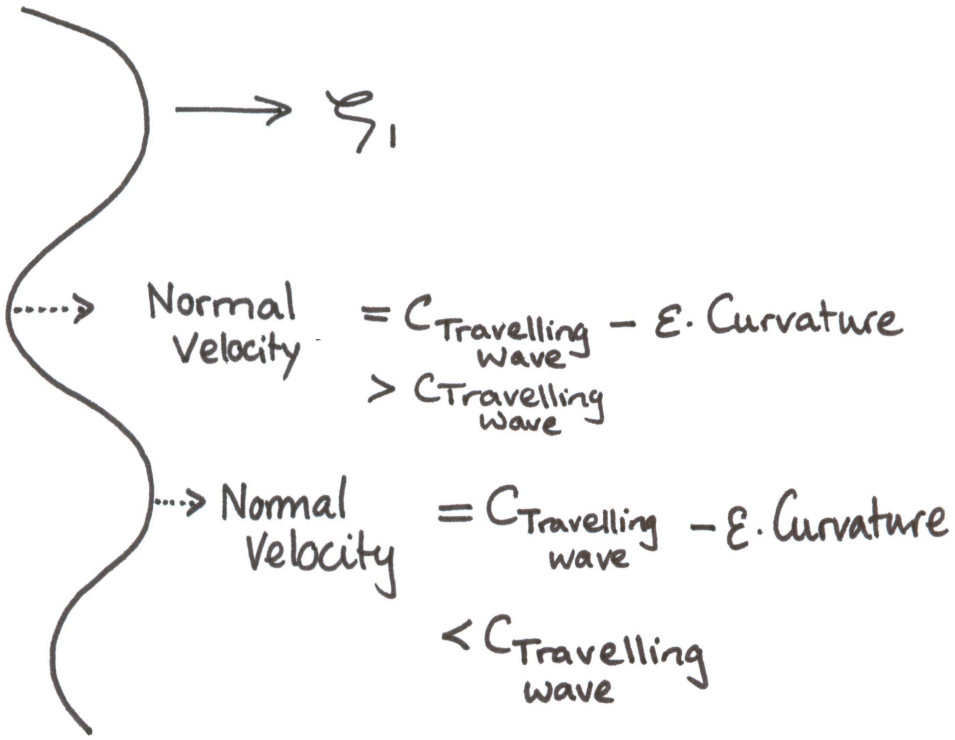

4.3 Target patterns

Target patterns are circular or spherical wavefronts which originate from a point. An example of a target pattern in the heart are the depolarisation waves which originate from the sino-atrial node (the pacemaker region). Further examples of target patterns are monomorphic ventricular tachycardia and Wolff-Parkinson-White disease. A numerical solution of the FitzHugh-Nagumo equations (using a cubic function for $f(v)$ with stable roots at $v = 0$ and $v = 1$) showing a target pattern is shown in figure 5. The initial conditions used were $v = 0$ when $r > r_0$ and $v = 1$ when $r < r_0$ (i.e. a circular region of tissue was excited).

We now demonstrate that circular wavefronts are solution of the eikonal-curvature equation (21). Consider a wavefront in the x-y plane. The radius $r(\theta, t)$ of the wavefront is a function of polar

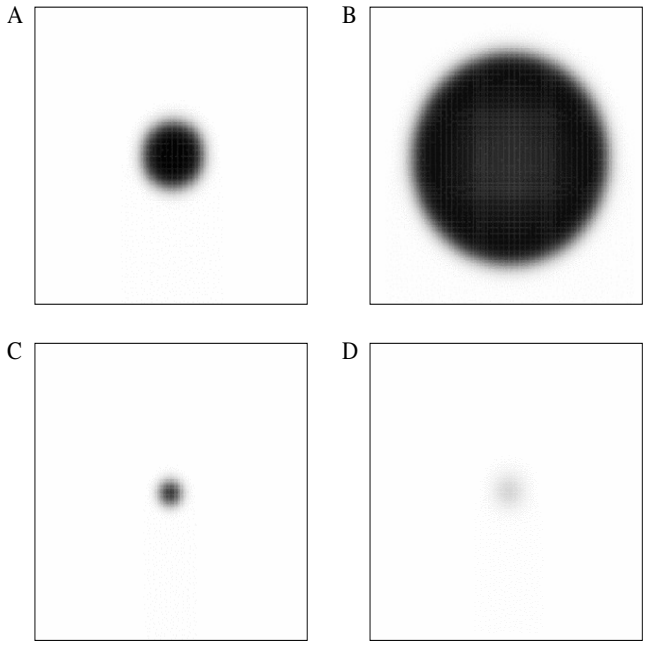

Figure 5: Solutions of the FitzHugh-Nagumo equations showing target patterns (white is v=0; black is v=1). When a large circular wavefront is excited (A), the wave propagates outwards (B). However, when a small circular wavefront is excited (C) the wave front decreases in size (D) due to curvature blocking.

angle θ, so the position $\mathbf{x}$ of the wavefront is

$$\mathbf{x} = \begin{pmatrix} r(\theta,t)\,\cos(\theta) \\ r(\theta,t)\,\sin(\theta) \end{pmatrix}. \tag{25}$$

The tangent vector $\mathbf{t}$ and normal vector $\mathbf{n}$ are then

$$\mathbf{t} = \begin{pmatrix} -r\sin(\theta) + r_\theta\cos(\theta) \\ r\cos(\theta) + r_\theta\sin(\theta) \end{pmatrix} \quad \text{and} \quad \mathbf{n} = \frac{1}{\sqrt{r^2+r_\theta^2}} \begin{pmatrix} r\cos(\theta) + r_\theta\sin(\theta) \\ r\sin(\theta) - r_\theta\cos(\theta) \end{pmatrix}. \tag{26}$$

Inserting (25) into the eikonal-curvature equation for a general wavefront in two-dimension (23) yields

$$r_t = c\frac{\sqrt{r^2+r_\theta^2}}{r} + \varepsilon\frac{rr_{\theta\theta} - 2r_\theta^2 - r^2}{r(r^2+r_\theta^2)}. \tag{27}$$

This is the eikonal-curvature equation in polar co-ordinates. Solutions of this equation which represent circular wavefronts will be of the form $r(\theta,t) = R(t)$, so

$$R_t = c - \frac{\varepsilon}{R} \tag{28}$$

If the initial circular wavefront is sufficiently large (i. e. $R(0) > R_c = \varepsilon/c$) the wave will expand outwards, however, if $R(0) < \varepsilon/c$ then the wavefront will collapse to the origin. This is an example of the phenomenon of *curvature blocking*, where wavefronts do not propagate if their curvature is too high. Figure 5A and B show a solution of the FizHugh-Nagumo equations where the initial circular wavefront is sufficiently large for the wavefront to expand outwards. However, when the initial circular wavefront is below a critical value the wavefront shrinks (figure 5C and D). This calculation suggests that the size of the sino-atrial node (pacemaker region) has to be sufficiently large for a wave to be excited. It should be noted that while the solution of (28) demonstrates the phenomenon of curvature blocking, it occurs when the curvature is $O(\varepsilon^{-1})$ so the asymptotic assumptions used to derive the eikonal-curvature equation are no longer valid. However, the qualitative behaviour of solutions of the FitzHugh-Nagumo equations (figure 5) are captured by the eikonal-curvature equation.

We have shown that there are solutions of the eikonal-curvature equation which are circular wavefronts. We shall now demonstrate that these wavefronts are geometrically stable using a linear stability analysis. Consider a small perturbation to the circular wavefront

$$r(\theta,t) \sim R(t) + \mu\tilde{r}(\theta,t), \tag{29}$$

where $\mu \ll 1$. A wavefront is geometrically stable if $\tilde{r}(\theta,t) \to 0$ as $t \to 0$ for all θ. Inserting (29) into (27) and taking the limit $\mu \to 0$ yields

$$\tilde{r}_t = \frac{\varepsilon(\tilde{r}_{\theta\theta} + \tilde{r})}{R(t)^2}. \tag{30}$$

Circular symmetry demands that $\tilde{r}(\theta) = \tilde{r}(\theta + 2\pi)$, which implies that solution must be of the form $\tilde{r} = \sum a_n(t)e^{in\theta}$ where n is an integer. Looking for solution of this form yields

$$\frac{da_n}{dt} = \frac{\varepsilon(1-n^2)}{R(t)^2}a_n. \tag{31}$$

The first thing to notice is that the $n = 0$ solution appears to be unstable. However, the coefficient for this solution can always be set to zero by choosing the initial condition $R(0)$ in the un-perturbed solution. The $n = 1$ solution is neutrally stable, which arises because the initial perturbation $\tilde{r}(\theta, 0)$ can shift the origin circular waves by an $O(\mu)$ distance.
Target patterns occur in both physiological conditions and in diseased states of the heart. One example of the target patterns are the depolarisation waves originating from the sino-atrial node which act as the pacemaker for the heart. An important question to ask is how large must the sino-atrial node be for the depolarisation wave to successfully transmit from the sino-atrial node into the atria. Normally the sino-atrial node is larger than the critical value $R_c(= \varepsilon/c)$. However in conditions such as hyperkalaemia, when the excitability of the tissue is greatly reduced, it is possible for the wave to fail to transmit from sino-atrial node (sino-atrial block). This will occur if the decreases in excitability (which increases ε) increases the critical radius R_c beyond the radius of the sino-atrial node. Other examples of target patterns are monomorphic ventricular tachycardia and Wolff-Parkinson-White disease.

4.4 Spiral waves

Spiral waves are self-replicating patterns which consist of a rotating spirals; see figure 6. They are important as they lead to re-entrant behaviour without pacemaking cells. Re-entrant behaviour is when one part of the tissue is continually re-excited. Spiral waves are thought to be the cause of polymorphic ventricular tachycardia. Instabilities in spiral waves can lead to them breaking-up forming multiple wavelets. This is a possible explanation for the breakdown of ventricular tachycardia into ventricular fibrillation which is fatal if not treated immediately. Scroll waves are the three dimensional analogue of spiral waves.

Figure 6 shows a solution of the FitzHugh-Nagumo equations exhibiting a spiral wave. The fact that spiral waves rotate means that spiral wave solutions are *periodic* in time. The mathematical description of spiral waves centres on the nature of *periodic* solutions of the Fitzhugh-Nagumo equations. We have previously considered *planar* periodic solutions of the FitzHugh-Nagumo equations (Example sheet 2, question 2.3). In particular, for a given wavelength, λ, the speed of the travelling wave, $c = \mathcal{C}(\lambda)$, can be determined. The relationship between the localised speed of the wavefront, and the speed of the planar periodic solutions is then given by the 2D Fitzhugh-Nagumo eikonal equation

$$\varepsilon\nabla \cdot \mathbf{n} + \mathbf{n} \cdot \frac{d\mathbf{X}}{dt} = \mathcal{C}(\lambda). \tag{32}$$

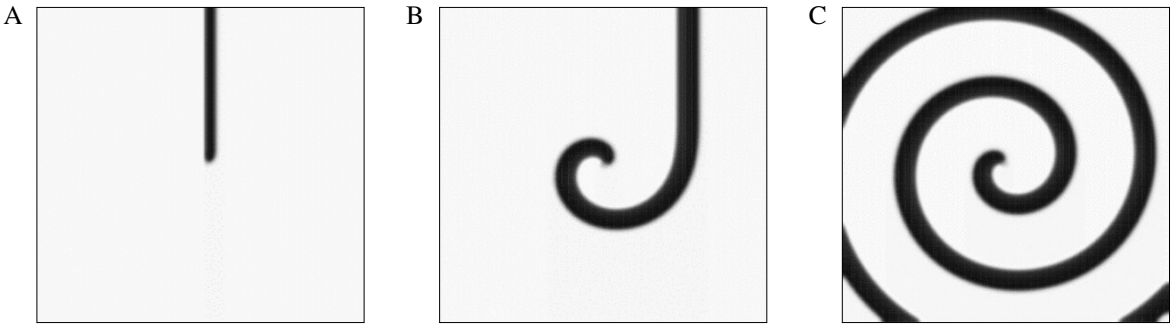

Figure 6: Solutions of the FitzHugh-Nagumo equations showing spiral waves (white is v=0; black is v=1). The initial conditions (A) is a plane wave in half the domain which wraps around a central core forming a re-entrant spiral waves (C) which continues to re-excite the tissue. In the centre of the domain is a core consisting of a small disk of 'dead tissue' (where $f(v) = 0$) which pins the spiral wave to the centre.

Suppose we consider the set of points

$$\begin{aligned} \mathcal{L} &\stackrel{def}{=} \{(X,Y)| \quad X = r\cos(\phi(r) - \omega t), \quad Y = r\sin(\phi(r) - \omega t), \quad r > 0\} \\ \lim_{r\to\infty} \phi'(r) &= \frac{2\pi}{\lambda}. \end{aligned} \tag{33}$$

Our aim is to show that these points constitute a front which is a solution of the 2D Fitzhugh-Nagumo eikonal equation (32). In particular, the front describes an outwardly propagating spiral wave, which asymptotically, as $r \to \infty$, corresponds to circular waves propagating outwards that locally are planar periodic solutions of the Fitzhugh-Nagumo equations of wavelength λ. **Our goal is to determine $\phi(r)$, ω and λ.**

4.4.1 Asymptotic form of spiral wave

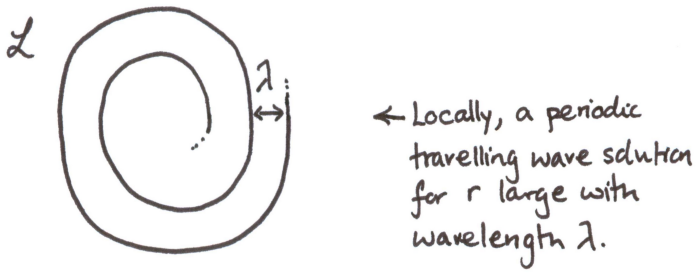

Consider equation (33) with r asymptotically large. Since

$$\lim_{r\to\infty} \phi'(r) = \frac{2\pi}{\lambda} \tag{34}$$

it follows, in the large-r limit, that increasing r by λ increases $\phi(r)$ by 2π and hence the spiral has undergone one revolution. The asymptotic spiral wave locally looks like a one spatial dimension periodic solution of the Fitzhugh-Nagumo equations of wavelength λ.

4.4.2 The eikonal equation

Similarly to the target pattern solution, we search for a solution of the eikonal equation in polar co-ordinates. However, instead of looking for a solution $r(\theta, t)$, we look for a solution of the form

$$\theta(r, t) = \phi(r) - \omega t, \tag{35}$$

so the position of the wavefront is

$$\mathbf{x} = \begin{pmatrix} r\,\cos(\phi(r) - \omega t) \\ r\,\sin(\phi(r) - \omega t) \end{pmatrix}. \tag{36}$$

Note that r is now used to parameterise the curve of the wavefront instead of θ which was used for target patterns. Inserting this expression into the eikonal-curvature equation (23) yields

$$c = \frac{\omega r}{\sqrt{1 + r^2\phi_r^2}} + \varepsilon \frac{r\phi_{rr} + r^2\phi_r^3 + 2\phi_r}{(1 + r^2\phi_r^2)^{3/2}} \tag{37}$$

Away from the core of the spiral the effect of curvature can be neglected, which gives a first order equation for ϕ

$$\phi_r = \left(\frac{\omega^2}{c^2} - \frac{1}{r^2}\right)^{1/2}. \tag{38}$$

This equation can be integrated when $r > c/\omega$ to give

$$\phi = \sqrt{\frac{r^2}{r_0^2} - 1} - \tan^{-1}\left(\sqrt{\frac{r^2}{r_0^2} - 1}\right) \tag{39}$$

where $r_0 = c/\omega$ (the integration constant just shifts the origin of time so is dropped). This is the equation of the involute of a circle of radius r_0. The involute of a circle can be drawn by tieing a pencil to the end of a thread in a cotton wheel and unwinding the thread. Note that this theory so far has yet to determine the frequency of the spiral wave. This is because the frequency is determined by the behaviour in the core of the spiral, as we now go on to examine.[1]

A condition on ω

[1]It should be noted that in the core of a spiral the curvature is $O(1/\varepsilon)$, so the assumptions used in deriving the eikonal-curvature equation are no longer valid. However, similar to the case of *curvature blocking* in target patterns, the eikonal-curvature equation successfully determines the qualitative behaviour of FitzHugh-Nagumo equations.

Suppose now we define $\psi = r\phi'$, $\psi' = d\psi/dr = r\phi'' + \phi'$. Then

$$\varepsilon \nabla \cdot \mathbf{n} = \varepsilon \frac{\psi' + \frac{\psi}{r}(1+\psi^2)}{(1+\psi^2)^{3/2}} = \varepsilon \frac{\psi'}{(1+\psi^2)^{3/2}} + \varepsilon \frac{\psi}{r(1+\psi^2)^{1/2}}.$$

Then the Fitzhugh-Nagumo eikonal equation is

$$\varepsilon \frac{\psi'}{(1+\psi^2)^{3/2}} + \varepsilon \frac{\psi}{r(1+\psi^2)^{1/2}} = c - \frac{\omega r}{\sqrt{1+\psi^2}}, \tag{40}$$

where $c = \mathcal{C}(\lambda) > 0$ is the travelling wave speed of the 1D planar waves, and λ is the wavelength observed locally as $r \to \infty$.
Consider equation (40) as $r \to \infty$. We have from equation (33) that $\psi = r\phi' \sim 2\pi r/\lambda$, as $r \to \infty$. Thus $\psi' \to 2\pi/\lambda$ as $r \to \infty$ and hence

$$\frac{\psi'}{(1+\psi^2)^{3/2}}\ , \quad \frac{\psi}{r(1+\psi^2)^{1/2}} \to 0 \quad \text{as } r \to \infty.$$

Consequently, for a solution to exist, we must have

$$c = \mathcal{C}(\lambda) = \lim_{r\to\infty}\left(\frac{\omega r}{\sqrt{1+\psi^2}}\right) = \frac{\omega\lambda}{2\pi} \qquad \text{i.e.} \qquad \omega = \frac{2\pi\mathcal{C}(\lambda)}{\lambda} \tag{41}$$

Thus we now have ω in terms of λ. To determine λ we consider the boundary conditions for equation (40).

Boundary conditions
We require $\psi \to 0$ as $r \to 0$ otherwise $\phi(r)$ is singular at the origin. However, having $\psi \to 0$ as $r \to 0$ is problematic. Note that (40) is equivalent to $\psi' = \frac{d\psi}{dq}/\frac{dr}{dq}$ where

$$\frac{d\psi}{dq} = -\psi(1+\psi^2) + \frac{cr}{\varepsilon}(1+\psi^2)^{3/2} - \frac{\omega r^2}{\varepsilon}(1+\psi^2), \qquad \frac{dr}{dq} = r. \tag{42}$$

The equilibrium point $(\psi, r) = (0, 0)$ is a saddle in the (ψ, r) phase plane. Hence the solution corresponding to the unstable manifold at the origin (pointing into $r > 0$) is required, otherwise the condition $\psi \to 0$ as $r \to 0$ cannot be enforced. To ensure the solution is on the unstable manifold one must additionally impose the condition

$$\psi'(r = 0) = c/(2\varepsilon) = \mathcal{C}(\lambda)/(2\varepsilon), \tag{43}$$

which can be deduced by considering the eigenvectors of the linearised matrix at $(\psi, r) = (0, 0)$.

Thus, we must solve the first order differential equation (40) subject to the *two* boundary conditions

$$\psi'(r = 0) = \mathcal{C}(\lambda)/(2\varepsilon), \qquad \psi'(r = \infty) = \frac{2\pi}{\lambda}. \tag{44}$$

Consequently, in general, we have an over specified number of conditions, and no solution exists. However, one can show numerically that for ε fixed, there is a unique value of λ for which both boundary conditions can be satisfied.

In summary, once λ is determined numerically, and

$$\omega = \frac{2\pi \mathcal{C}(\lambda)}{\lambda}$$

the set of points

$$\begin{aligned} \mathcal{L} &\stackrel{def}{=} \{(X,Y)| \quad X = r\cos(\phi(r) - \omega t), \quad Y = r\sin(\phi(r) - \omega t), \quad r > 0\}, \\ \lim_{r\to\infty} \phi'(r) &= \frac{2\pi}{\lambda} \end{aligned}$$

constitutes the time dependent position of an excitation front which solves the $2D$ Fitzhugh Nagumo eikonal equation provided $\psi = r\phi'(r)$ satisfies

$$\varepsilon \frac{\psi'}{(1+\psi^2)^{3/2}} + \varepsilon \frac{\psi}{r(1+\psi^2)^{1/2}} = c - \frac{\omega r}{\sqrt{1+\psi^2}}, \qquad c = \mathcal{C}(\lambda)$$

subject to suitable boundary conditions.